

HARD X-RAY AND WIDE FOCUSING TELESCOPES

NASA Grant NAG5-5095

INTERIM
10-89
380 448

Annual Report

For the Period 22 November 1996 through 21 November 1998

Principal Investigator
Dr. Paul Gorenstein

September 1998

Prepared for:

National Aeronautics and Space Administration
Goddard Space Flight Center/Wallops Flight Facility
Wallops Island, VA 23337

Smithsonian Institution
Astrophysical Observatory
Cambridge, Massachusetts 02138

The Smithsonian Astrophysical Observatory
is a member of the
Harvard-Smithsonian Center for Astrophysics

The NASA Technical Officer for this grant is William B. Johnson, Code 810.0, NASA Goddard Space Flight Center, Wallops Flight Facility, Wallops Island, VA 23337.

1 INTRODUCTION

This is the first annual report for NASA Grant NAG5-5095. Substantial progress was made on each of the three items of our statement of work, (1) epoxy replication of flat reflectors as substrates for multilayer reflectors, (2) deposition of multilayer reflecting layers upon those substrates followed by an evaluation of their performance in an 8 keV X-ray beam. As before, superpolished substrates which were not separated was included as a control. The final item, (3), design and construction of our own DC magnetron sputtering chambers. This includes a small R&D chamber and a large chamber that can accommodate two linear cathodes whose purpose is to coat the inside surface of conical shell reflectors. Each of these SOW items is discussed below.

2 REPLICATION OF SUBSTRATES FOR MULTILAYER COATINGS

Our collaborative program with O. Citterio of the Brera Observatory continued. SAO provided the master and all materials and took responsibility for the X-ray testing while replication was performed at Brera. We repeated our tests of the comparative merits of carbon and gold as separation agents in replication. As in the previous tests, we had 50 layers of a nickel-carbon multilayer deposited on each of the substrates at the National Institute of Science and Technology. Performance was evaluated by measuring the reflectivity of an 8 keV beam as a function of angle and measuring the amplitude and width of a series of Bragg like reflection peaks through the fifth order. Previously we had found that a substrate separated with carbon had a smoother surface than one separated with gold that had been deposited by e-beam evaporation. The comparison of gold with carbon was repeated. However this time we added substrates where gold was deposited by sputtering as well as by e-beam evaporation. Furthermore, as the use of carbon as a separation agent is novel, at least in the open literature, we wanted to test the reproducibility of the carbon results of the previous year.

Our results are reported in a paper presented at the 1998 annual meeting of the SPIE. That paper is reproduced in Appendix A. In summary, we found that although the smoothness of a carbon separated substrate was reproducible, the ease of separation was not. We had repeated the carbon deposition by having it done at the same commercial facility and with the same sputtering target. However, the separation properties were quite different this time. The force required to separate the replica from a carbon coated mandrel was much larger than previously. It was large enough to shatter the carbon layer in one of the two samples that were prepared. We were not able to identify the reason for the lack of reproducibility. All factors and conditions appeared to be the same. To elucidate the matter, both SAO and Brera deposited carbon layers on glass flats with our own sputtering systems. Separation tests were performed on all substrates. Both the SAO and Brera deposited carbon layers required excessive force to separate the replica from the mandrel. Investigation of why the carbon results are not reproducible will continue in our own facilities.

On the other hand we were happy to observe that sputtered gold is superior to evaporated gold. While a replica separated with carbon still has the smoothest surface of all, sputtered gold may be good enough to satisfy our requirements. With our present multilayer coatings the overall performance appears to be more influenced by interface diffusion of the heavy and light materials than

by the roughness of the underlying substrate. Unlike carbon the behavior of gold as a separation agent has been well studied and is reproducible. Separation forces were similar for the evaporated and sputtered gold. This conclusion may change if we succeed in reducing interface diffusion by substituting compound materials for the pure element layers, e.g. W-C/C for W/C. In that case, the underlying roughness of the substrate which propagates through the layers may become the limitation.

3 CONSTRUCTION OF SPUTTERING CHAMBERS

During the past year we made considerable progress in the design and construction of two deposition facilities with DC magnetron sputtering cathodes. Complementary funding from the Smithsonian Institution made a substantial contribution to this project. The first, the smaller chamber, can deposit multilayer coatings upon flat substrates up to 3 in. x 3 in. It is intended primarily for research and development of coating materials and investigation of optimal coating conditions. The second is much larger and can coat a variety of substrates arrayed in a cylindrical geometry up to a diameter of 18 inches and 24 inches long. Its primary purpose is depositing multilayer coatings on actual hard X-ray telescopes including the interior surface of an integral cylinder, the approach we favor for higher energy X-ray telescopes. However, it can coat any array of segments, linear or curved that approximates a cylindrical geometry. Both chambers are now operational and coating studies are proceeding.

Photos of the two chambers are shown in a paper by Romaine et al, 1998 that was presented at the 1998 annual SPIE meeting. It is reproduced as Appendix B. The large cylindrical chamber employs 26" long cathodes of a custom design produced by Angstrom Sciences. These cathodes were plagued by a number of manufacturing defects such as leaks in water lines and incorrect spacings between of high voltage and grounded components. Most of these were rectified serially but a considerable loss of time. Corrective action is ongoing while the systems are functional but at less than full efficiency.

4 PRODUCTION OF MULTILAYER COATINGS IN OUR CHAMBERS

Several multilayer coatings were produced in both chambers. This was preceded by a series of single coating depositions to calibrate the rate of deposition as a function of current. We also experimented to find optimum values of argon pressure and deposition rates for both chambers.

The multilayer coatings we produced were of acceptable quality. Improvement is expected as we refine the operating parameters and experiment with new materials.

Results from these depositions were presented at the annual SPIE meeting in a paper by Ivan et al. This paper is reproduced in Appendix C.

APPENDIX A

Progress in Replication of Substrates for Multilayer Coatings

S. Romaine^{1,2}, J. Everett¹, R. Bruni¹, A. Ivan^{1,3}, P. Gorenstein¹

¹Harvard-Smithsonian Center for Astrophysics
60 Garden Street, Cambridge, MA 02138

²Bunting Institute, Radcliffe College
34 Concord Ave, Cambridge, MA 02138

³MIT
Mass Ave, Cambridge, MA 02138

M. Ghigo, F. Mazzoleni, O. Citterio

Osservatorio Astronomico di Brera-Milano
Via E. Bianchi, 46 - 22055 Merate, Italy

J. Pedulla

National Institute of Standards and Technology
Physics Laboratory
Gaithersburg, MD 20899

Abstract

Studies are being carried out to compare the performance of several different separation materials used in the replication process. This report presents the results obtained during the second year of a program which consists of replicating smooth, thin substrates, depositing multilayer coatings upon them, and evaluating their performance. Replication and multilayer coatings are both critically important to the development of focussing hard X-ray telescopes that function up to 100 keV. The activities of the current year include extending the comparison between sputtered amorphous carbon and evaporated gold to include sputtered as well as evaporated gold. The figure of merit being the smoothness of the replica which has a direct effect on the specular reflectivity. These results were obtained with epoxy replication, but they should be applicable to electroformed nickel, the process we expect to use for the ultimate replicated optics.

Keywords: X-ray Telescopes, Multilayers, Replicated Substrates

1 INTRODUCTION

As part of a program to develop multilayer grazing incidence optics for a hard X-ray telescope, replication is being investigated for the production of light weight, high resolution cylindrical optics. A previous study [1] reported the results for replicated substrates where the separation material was DC magnetron sputtered carbon and E-gun evaporated gold; that study also reported results for control samples (i.e. multilayers deposited directly on the bare substrate, no replication). We have now extended this study to include DC magnetron sputtered gold as the separation material in the replication process. In addition we have fabricated new samples with the DC magnetron sputtered carbon and E-gun evaporated gold as the separation material to make a direct comparison with previous results. In all cases, superpolished fused silica substrates were used as masters to produce epoxy replicated surfaces onto float glass. After the epoxy replication, nickel/carbon multilayers were deposited onto the float glass and the specular X-ray reflectivity measured. The multilayers were deposited using dual ion beam assisted deposition at low ambient pressure ($\approx 10^{-4}$ Torr). The results from four epoxy replicated samples are reported in this paper.

Results of X-ray reflectivity measurements of the multilayers on the 3 different separation materials is reported below and compared with previous results for similar samples. Results of surface roughness from AFM measurements and from modelled data is also given below; it has been shown [2] that a surface roughness of less than 5 Å is needed for good X-ray reflectivity performance up to 100 keV. The DC magnetron sputtered gold replicated samples are similar in quality to the DC magnetron sputtered carbon replica samples, the E-gun evaporated gold replica samples show inferior and more variable sample to sample performance.

We plan to extend this study to electroformed replicas in the near future. Success in the electroforming process would make accessible the telescope technology developed for SAX, JET-X, and XMM. However, it requires that the mandrel surface be conducting in order for the nickel to adhere. Consequently, we are experimenting with additional metallic layers over the carbon in order to bond to electrodeposited nickel. Replication trials will be carried out on both flat and cylindrical shell substrates.

2 SAMPLES

Dual ion beam assisted deposition was used to deposit multilayers on all samples discussed here. Nominal d-spacing and γ (ratio between nickel and period) for the Ni/C multilayers is 40 Å and 0.4, respectively. The number of bilayers deposited was 50 in all cases. E-gun evaporated gold was used as the separation material on 2 of the samples, DC magnetron sputtered gold was used on the third sample and DC magnetron sputtered carbon was used on the fourth. The thickness of the separation agent in all cases was nominally 2000 Å. The list of samples is shown in table 1.

3 MEASUREMENTS

3.1 X-ray Reflectivity Measurements

Figure 1 shows the X-ray reflectivity data for all samples. Although 3 Bragg peaks are clearly visible for each sample, there is a noticeable difference in the peak intensities among the different samples. Overall, the DC magnetron sputtered carbon and gold performed noticeably better than the E-gun evaporated gold. We also note that the specular reflectivity of the multilayers on the 2 E-gun evaporated gold replica samples varies considerably between samples 474 and 514.

The results agree with previous results in that the DC magnetron sputtered carbon yields a higher reflectivity than do the E-gun evaporated gold samples. This study shows that the DC magnetron sputtered gold performs approximately as well as the DC magnetron sputtered carbon.

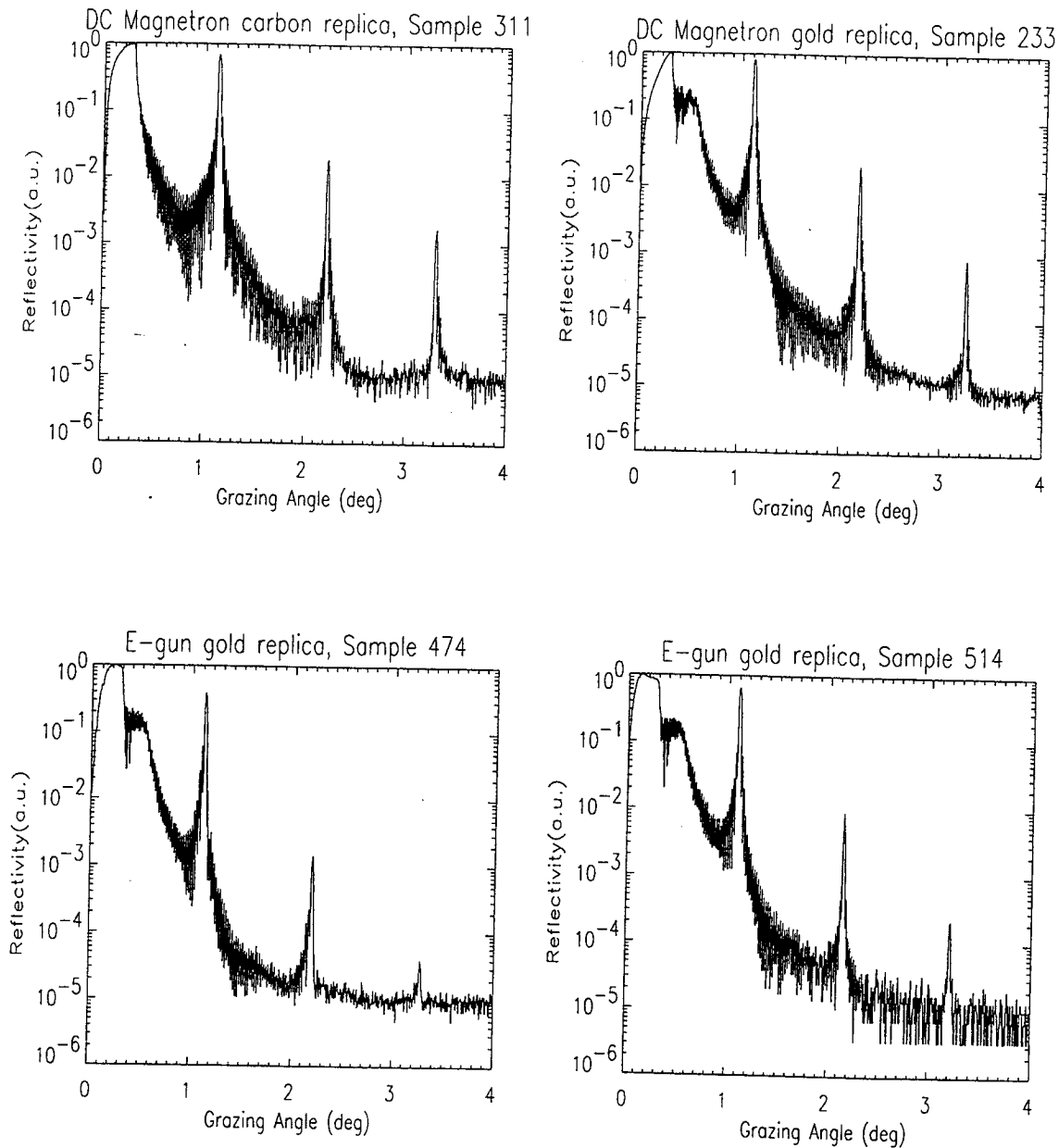


Figure 1: Specular reflectivity vs. grazing angle for each of the 4 different samples. All data was taken at 8 keV. Bragg peaks are clearly visible.

3.2 Microroughness Data

It is well known that surface microroughness has a strong effect on the intensity of the grazing incidence specular reflection [3, 4]. This effect becomes more pronounced the higher the energy of incident photons

(i.e. the smaller the grazing angle). Table 1 gives the interface roughness of the multilayer as calculated from fitting the model to the data, and also lists the surface microroughness results (from atomic force microscopy) before depositing the multilayer film. The AFM surface microroughness of the replica is less than that of the coated master for both of the sputtered samples. The replica surface that is measured is the 'separated surface', i.e. the layer that was in direct contact with the superpolished master. The 'AFM master' surface referred to in the table is the top surface of the deposited layer (gold or carbon). The calculated (modelled) interface microroughness of the multilayers shows a consistent difference of 1\AA between the DC magnetron sputtered samples and the E-gun samples, (4\AA for the DC magnetron sputtered samples and 5\AA for the E-gun samples).

Figure 2 presents two reflectivity vs. grazing angle plots for 4\AA μr and 5\AA μr models. The model parameters used here were the same as those discussed above, i.e., $N=50$, $d=40\text{\AA}$ and $\gamma = 0.36$. A clear difference can be seen, especially in the intensity of the second and third order Bragg peaks, as was seen in the data in figure 1, indicating a clear improvement in specular reflectivity with an improvement from 5 to 4\AA in the interface microroughness.

Surface Microroughness (\AA)				
Sample Number	Sample Description	AFM Master	AFM Replica	post-coat (model)
311	DC mag sputtered carbon replica	0.9-2.2	1	4/4.5
233	DC mag sputtered gold replica	8-11	1-1.7	4/4.5
474	E-gun gold replica	3-7	2-9	5.7/5.7
514	E-gun gold replica	6-13	3.5-5	5/5.5

Table 1: X-ray modelled and AFM measured microroughness data for the 4 samples discussed in the text. The AFM data given here is for 0.5 , 1.0 and $10.0\ \mu$ scan lengths and for 2 different areas for each sample. The model data is from fits to the 8 keV data. The 'AFM master' column is the AFM data for the *coated* master.

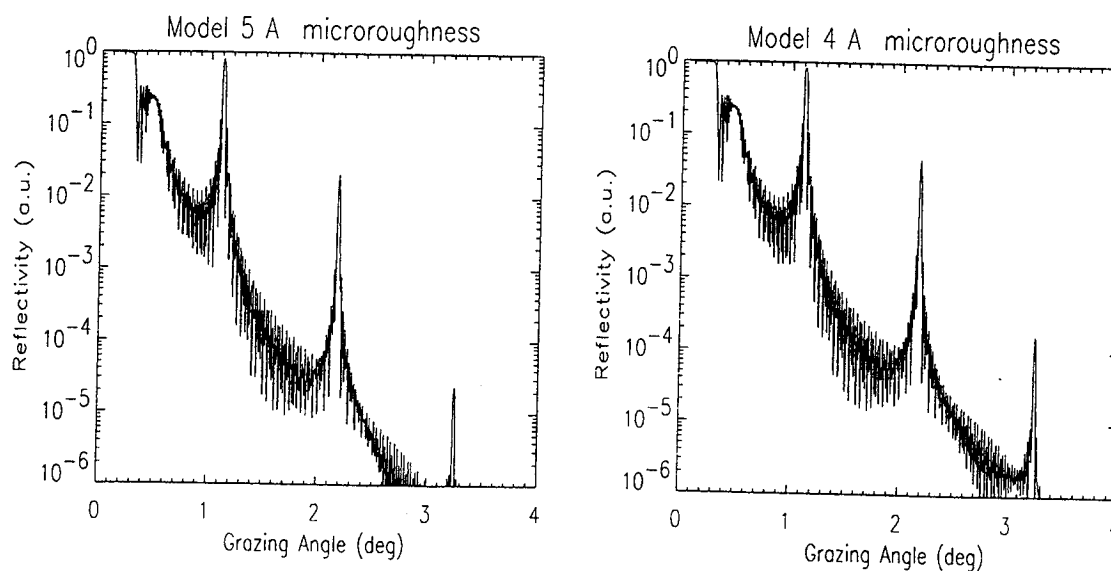


Figure 2: Model for specular reflectivity vs. grazing angle using an interface roughness of 5\AA (left plot) and 4\AA (right plot).

4 DISCUSSION and CONCLUSIONS

The quality of the multilayers deposited on DC magnetron sputtered carbon replicas, DC magnetron sputtered gold replicas and E-gun evaporated gold replicas has been assessed and the results have been compared with our previous studies. Specular reflectivity data at 8 keV was evaluated to compare the intensity of Bragg peaks and the modelled microroughness of the interfaces. The modelled interface roughness for the 2 DC magnetron sputtered samples, 233 and 311, is approximately 1 Å less than that of the E-gun samples, 474 and 514 (4Å vs. 5Å). These results agree with those reported earlier [1] which showed the performance of the DC magnetron sputtered carbon replicas to be superior to that of the E-gun gold replicas. The results from sample 474 were very similar to the earlier results reported for E-gun replicas. Sample 514, also an E-gun replica sample, although considerably better than the other E-gun samples still did not perform so well as the DC magnetron sputtered replicas.

The quality of the DC magnetron sputtered carbon in this study did not reproduce the same good separation properties (i.e. easily separable) as the carbon used in the previous study. We have not yet identified the cause of this difference. However, since the performance of the DC magnetron sputtered gold was of equal quality to the carbon, and since gold is easily separable and its behavior more reproducible, it is less imperative to resolve the carbon separation issue.

The combined results of our studies indicate that 4Å is the 'intrinsic' microroughness of the Ni/C multilayer interface, even if the surface microroughness of the starting substrate is 1Å. The results also indicate that the DC magnetron sputtering process produces a better quality material than does E-gun evaporation for the replication process.

5 ACKNOWLEDGEMENTS

We wish to thank Atkinson Systems of Hudson, NH for providing the DC magnetron carbon coatings. This work was supported in part by NASA contracts NAG8-1194 and NSG-5138 and the Bunting Institute.

References

- [1] S. E. Romaine, et al. 1997, "Application of Multilayer Coatings to Replicated Substrates", Proc. SPIE, **3113**, p.253(1997).
- [2] K.D.Joensen et al., "Medium-sized grazing incidence high energy X-ray Telescopes employing continuously graded multilayers", Proc. SPIE, **1736**, p.239(1992).
- [3] A. M. Clark, et al., 1996, "Correlation Between X-ray Reflectivity Measurements and Surface Roughness of AXAF Coated Witness Samples," Proc. SPIE, **2805**, p.268(1996).
- [4] D.L. Windt et al., "Surface Finish Requirements for soft X-ray Mirrors", Applied Optics **33**, 2025-2031 (1994).

APPENDIX B

Characterization and Multilayer Coating of Cylindrical X-ray Optics for X-ray Astronomy

S. Romaine^{1,2}, J. Everett¹, R. Bruni¹, A. Ivan^{1,3}, P. Gorenstein¹

¹Harvard-Smithsonian Center for Astrophysics
60 Garden Street, Cambridge, MA 02138

²Bunting Institute, Radcliffe College
34 Concord Ave, Cambridge, MA 02138

³MIT
Mass Ave, Cambridge, MA 02138

Abstract

We are engaged in a program to develop focusing hard X-ray optics for future X-ray astronomy missions. Optics are being developed to focus X-rays up to and beyond 80 keV. Emphasis is on the multilayer coating of integral cylindrical optics which will provide the highest spatial resolution. A chamber geometry has been designed to allow the uniform coating of the inside surface of integral cylinders. The building and testing of this system has taken place over the past year. Linear DC magnetron cathodes are used to sputter the multilayer films. Initial results from both longitudinal and azimuthal uniformity coating tests are presented.

Keywords: X-ray Telescopes, Multilayers, X-ray optics

1 INTRODUCTION

This past year a coating chamber has been designed and built with DC magnetron sputtering capability with particular emphasis on coating the inside surface of integral cylindrical optics. Our project goals are two-fold: (1) to assess replicated substrates to find the 'best' replication technique [1] and (2) to coat and test an integral cylindrical optic with graded d-spaced multilayers. This work is being carried out as part of the effort to design the hard X-ray telescope for the Constellation X-ray Mission [2].

2 EXPERIMENTAL DESIGN

Figure 1a is a photo of the chamber that has been built for this study. It's dimensions are approximately 44" high x 22" diameter; it is cryopumped and has a base pressure of 1×10^{-7} Torr. The cathodes used in this design are 26" long linear cathodes, one of which can be seen in figure 1b. There are 2 cathodes mounted back to back in the center of the chamber. Once the optic is loaded into the chamber, the cathodes

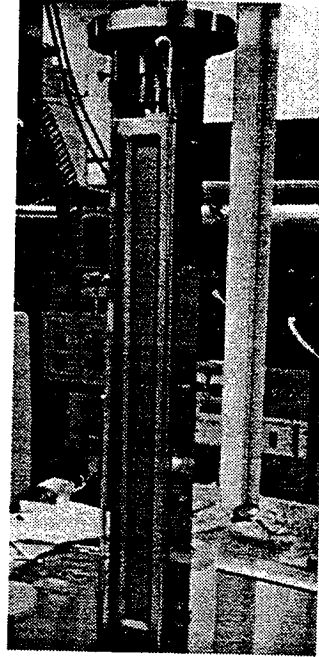
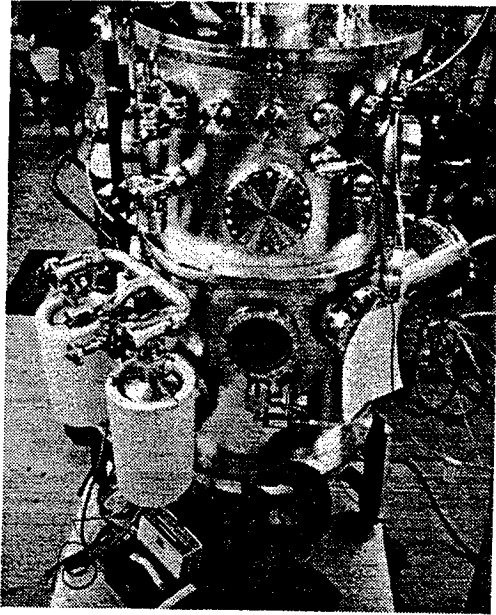


Figure 1: The figure on the left (fig. 1a) shows the chamber which was designed for sputtering multilayer coatings onto the inside surface of integral cylindrical optics. The photo on the right (fig. 1b) is a view of the linear cathode used in the chamber. Target height is 26", target width is 1.5".

are positioned inside the optic which rotates about the cathode to coat the inner surface of the 'cylinder'. Each target can be shuttered such that only one cathode is sputtering onto the optic at a given time.

2.1 Coating Surrogate

The characterizing of flat substrates is simpler than the characterization of integral cylindrical substrates and for this reason all the initial coating tests have been carried out on silicon wafers. To coat these flats such that they are representative of a true cylindrical surface, a coating surrogate was fabricated as shown in figure 2. This surrogate is a stainless steel cylinder with several 3inch diameter holes cut in the surface so that a flat substrate such as a silicon wafer can be mounted in the hole and coated to represent the inside surface area of the cylinder. Having several substrates mounted along the length of the surrogate provides samples to test the linear uniformity of the process; the array of substrates around the circumference provide samples for a check of the azimuthal uniformity. Figure 2b gives a view of the chamber as the cathode assembly is being lowered down into the surrogate optic prior to the start of a coating run.

3 RESULTS and DISCUSSION

The target materials purchased for these coating studies included tungsten, silicon, carbon and nickel. Initial tests were run with tungsten and carbon targets. The tests for deposition rates for given power, src-substrate

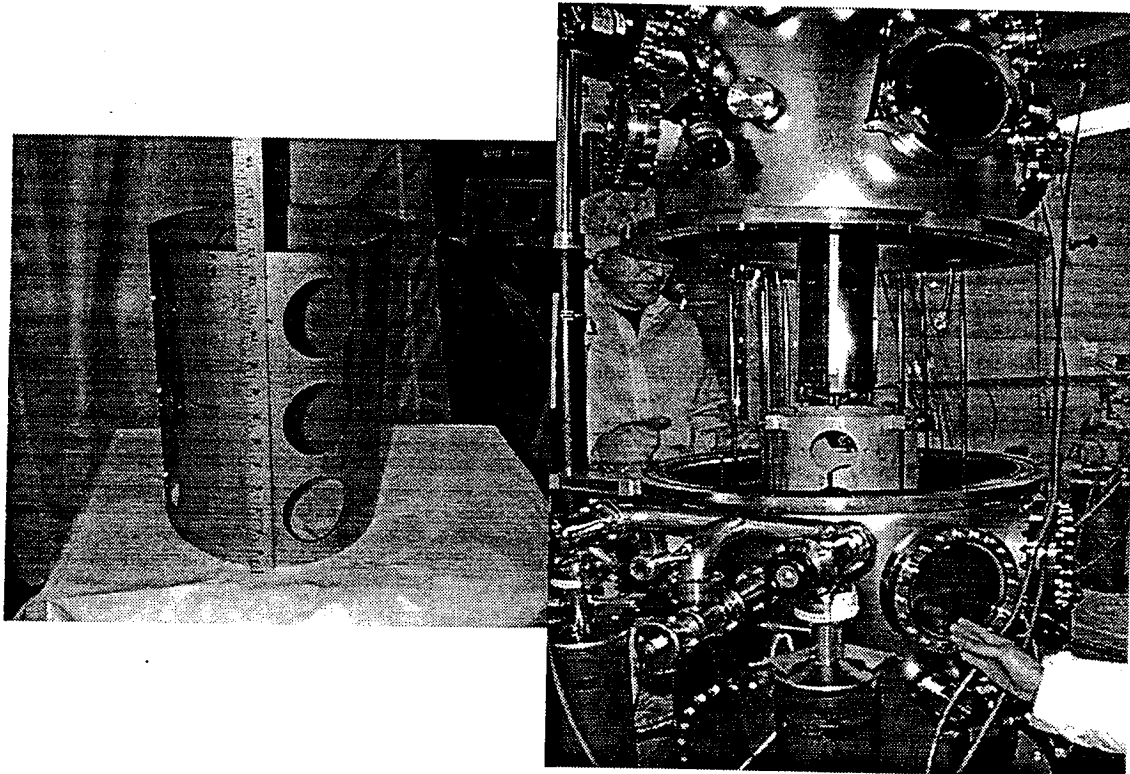


Figure 2: The figure on the left (fig. 2a) is a view of one of the surrogates fabricated for coating tests. The height is 13", diameter is 11". Three inch diameter mounting holes allow flat substrates to be coated so they are representative of the cylindrical surface. The photo on the right (fig. 2b) is a view of the chamber as the cathode assembly is being lowered down into the inside of the surrogate.

distance, etc. have only recently been completed and the first W/C multilayer ($N=20$ bilayers) was deposited this past week. Although several silicon wafers were coated during this first multilayer run, reflectivity results from only one wafer are complete at this time. A reflectometer is currently being built in our laboratory for measurements of these samples, but it will not be completed for several weeks. We were fortunate to have access to a reflectometer at Rome Laboratories to measure one sample before the conference. Figure 3a and 3b give 2 plots of reflectivity vs. grazing angle for 8 keV incident energy. Figure 3a is data from the first W/C multilayer sample fabricated in the cylindrical optic chamber. The plot in figure 3b is data from one of the multilayer samples fabricated in the R&D chamber which was built for coating flat substrates [4]. Both samples were fabricated using the same parameters: $N=20$ bilayers, $d=97 \text{ \AA}$, $\gamma = 0.26$. The solid line in each plot is the modelled fit to the data. The model for figure 3a has a microroughness of 6 \AA for all interfaces, the model for figure 3b has a microroughness of 6 \AA for the W/C interfaces and a microroughness of 2.5 \AA for the C/W interfaces. As discussed in an earlier paper [5] such a change in microroughness effects the intensity of the Bragg peaks.

The data in figure 3a also has low intensity 'peaks' between the main Bragg peaks. These extra peaks may be due to a variation in the layer thickness over the 20 layers. Computer control for the shutter motion is just now being installed; this sample was fabricated using manual shutter control which may have introduced a slight variation in the layer to layer thickness. No attempt was made to model a variation in layer thickness. The R&D chamber is totally computer controlled and has good control over layer thickness as seen from both reflectivity measurements and from TEM analysis. In addition, two different facilities were used to measure the 2 different samples shown here. The sample in figure 3a was measured with a setup

whose resolution was a factor of 5 worse than the setup used to measure the sample shown in figure 3b. This difference in resolution contributes to the difference in the sharpness of the Bragg peaks.

The first tests we hope to complete after installing the computer control will be a study of the linear and azimuthal uniformity of constant d-spaced multilayers fabricated using the coating surrogate.

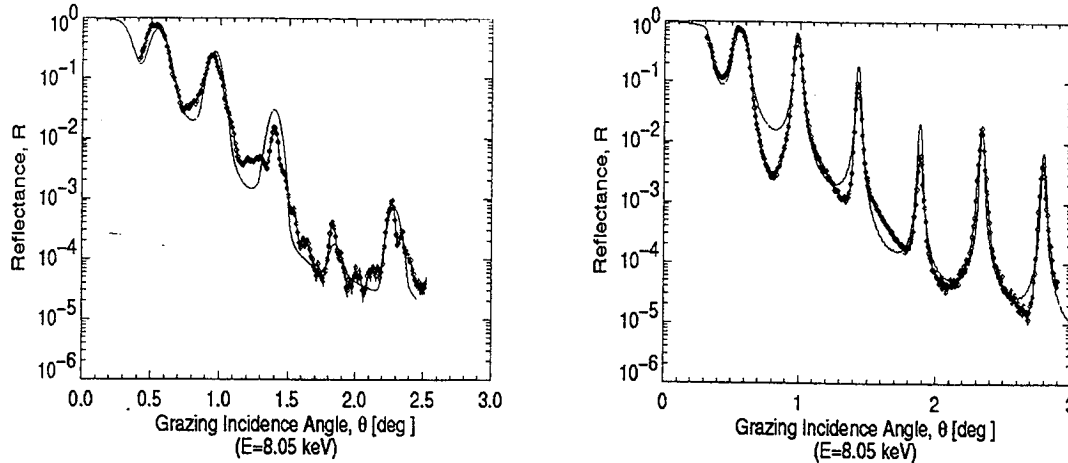


Figure 3: Plot of reflectivity vs. grazing angle for the first multilayer sample fabricated and tested in the cylindrical optic chamber. Solid line shows the results from a fit to the data. Incident energy was 8 keV. The plot on the right (fig. 3b) is a similar plot for a sample fabricated in the R&D chamber. Both samples used the parameters: $N=20$ bilayers, W/C , $d=97$ Å, $\gamma=0.26$.

4 ACKNOWLEDGEMENTS

We wish to thank Dr. Alvin Drehman at Rome Laboratories, Hanscom Air Force Base for the use of his reflectometer; the software used to model the data was provided by Dr. David Windt of Lucent Technologies [3]; we wish to thank Kyung Byun of Harvard University for much of the work in presenting the figures. This work was supported in part by NASA contracts NAG8-1194 and NSG-5138 and the Bunting Institute.

References

- [1] S. E. Romaine, et al. 1997, "Application of Multilayer Coatings to Replicated Substrates", Proc. SPIE, **3113**, p.253(1997).
- [2] N.E. White and H.D. Tananbaum, "The Constellation X-ray Mission", <http://constellation.gsfc.nasa.gov/>
- [3] D.L. Windt, "IMD version 4.0", <http://www.bell-labs.com/user/windt/idl/imd/index.html>
- [4] A. Ivan, et al. 1998, "Characterization of graded d-spacing multilayers for hard X-ray telescopes", Proc. SPIE, this volume.
- [5] S. E. Romaine, et al. 1998, "Progress in Replication of Substrates for Multilayer Coatings", Proc. SPIE, this volume.

values are typically 5-6 Å. This is probably due to diffusion at the interface and possible compound formation. The surface microroughness for sample CW28 was 6 Å rms as determined by AFM. The IMD fit yielded 8 Å rms, in good agreement with AFM, considering that the fit was varying many parameters and that the AFM and X-ray reflectivity measurements cover different spatial frequency ranges. The reflectivity scans clearly indicate different structures in samples CW26 and CW27, possibly due to a different target to substrate distance. Sample CW28 shows a "splitting" of the second and third Bragg peaks. The model for the fit considered that the first 20 bilayers have a different spacing than the next 20 bilayers, but this approach is only partially successful. Overall, the series of constant d samples showed that the control of the process is fairly good and that the reflectivity scans offer structure data in agreement with the design. More structural information is expected from TEM and AES analysis.

The graded d spacing sample designs were selected from an IMD-based simulation study for C/W multilayers with N=40 and 50. The thickness of each layer was chosen to vary with the layer position in the stack according to a power law [3]:

$$z(i) = \frac{a}{(b+i)^{0.25}}$$

where a and b are parameters, and i is the layer index number (i=1 for the topmost layer, N for the bottom layer).

Samples CW30 and CW31 have an identical design, with N=40, $\gamma=0.444$, and d graded from 161 Å at the top to 36 Å at the substrate. Sample CW32 has N=50, and γ as well as d are variable throughout the multilayer stack (see Table I). Both designs were intended to increase the reflectivity at small grazing angles for a range of X-ray energies from 10 to 80 keV. Fig. 8 shows reflectance vs. energy for CW32 at 5 arc-min grazing incidence and illustrates the effect of graded d structures on increasing the bandpass: up to 50 keV, the reflectance has only a narrow dip and is more than 80% for most of the energies.

Figures 4-6 present the reflectivity scans at 8.048 keV for these graded d samples. Again, there is a notable difference between the twin samples CW30 and 31, possibly due to different base pressures (3×10^{-7} T and 1×10^{-7} T, respectively). The fit is better for CW30. AFM surface microroughness measurements showed a value of 1.5 Å for CW30 (Fig. 7) and 2.0 Å for CW31, consistent with the values from the reflectivity data fit. The interfacial roughness/diffuseness from the fit is quite high: 10 Å, supporting the interdiffusion hypothesis.

Sample CW32 (N=50) has a reasonably good fit, but although the fitted d values are close to the design values, the trend for γ values is reversed.

Table I
Structure parameters (design vs. fit) for a set of constant and variable d spacing multilayers

Sample #	N (bilayers)	d (from deposition rate)	d(from reflectivity fit)	γ (deposition rate)	γ (reflectivity fit)
CW25	10	185 Å		0.324	
CW26	20	92.5 Å	113	0.324	0.254
CW27	20	92.5 Å	95.5	0.324	0.250
CW28	40	46.25 Å	51	0.324	0.203
CW30	40	161 Å (top)-36 Å (bottom)	160 Å (top) -36 Å (bottom)	0.444	0.368 (avg.)
CW31	40	161 Å (top)-36 Å (bottom)	180 Å (top) -36 Å (bottom)	0.444	0.366 (avg.)
CW32	50	137 Å (top)-30 Å (bottom)	126 Å (top) -28 Å (bottom)	0.617 (top) - 0.5 (bottom)	0.340 (top)- 0.439 (bottom)

3. CONCLUSIONS

The work presented here is a preliminary step in a program to coat integral cylindrical optics with graded d spacing multilayers. The samples presented are correlated with and preceded sputtering tests of depositing C/W multilayers in another, larger high vacuum chamber with 26 in. long cathodes. After identifying process parameter values that optimize single layer coatings, we continued with single d spacing multilayer runs for which the interpretation of reflectivity data is straightforward. The analysis showed that the control of the process is fairly good and the reflectivity data are correlated with the expected structure. The coatings based on a graded d spacing design confirmed the previously known effect of broadening the reflection passband and showed that the specular reflectance scans could be fit well by the model. Some discrepancies indicate that perfect reproducibility of the runs still needs more accurate control of certain deposition parameters (base pressure, target-to-substrate distance, etc). More analysis is required to describe the interface roughness/diffuseness and TEM and AES work is in progress for this purpose. The procedures used for the fabrication and characterization of the trial C/W samples will be used for the next graded d spacing coating studies based on other reflector/spacer material combinations (W/Si, Ni/C, W/B₄C, Pt/C).

4. ACKNOWLEDGEMENTS

We would like to acknowledge the help of the technical staff at CMSE-MIT, in particular to Libby Shaw and Mike Frongillo. The reflectivity data analysis was performed using the IMD v.4.0 software package developed by David L. Windt, Bell Laboratories, Lucent Technologies.

The X-ray reflectivity measurements were performed at two locations: Physics Department, Harvard University, and Physics Department, Boston University. We are indebted to Prof. Peter Pershan and Prof. Karl Ludwig for allowing us to use their X-ray instruments.

This work made use of the MRSEC Shared Experimental Facilities supported by the National Science Foundation under award number DMR94-00334.

5. REFERENCES

1. S.E.Romaine, R.J.Bruni, J.Everett, A.Ivan, P.Gorenstein, "Characterization and multilayer coating of cylindrical x-ray optics for x-ray astronomy", oral presentation, SPIE's 43rd Annual Meeting, San Diego, 1998.
2. D.L.Windt, "IMD version 4.0", <http://www.bell-labs.com/user/windt/idl/imd/index.html>
3. K.D.Joensen, F.E.Christensen, H.W. Schnopper, P.Gorenstein, J.Susini, P.Høghøj, R.Hustache, J.Wood, K.Parker, "Medium-sized grazing incidence high-energy x-ray telescopes employing continuously graded multilayers", Proc. SPIE, 1736, pp.239-248, 1993.

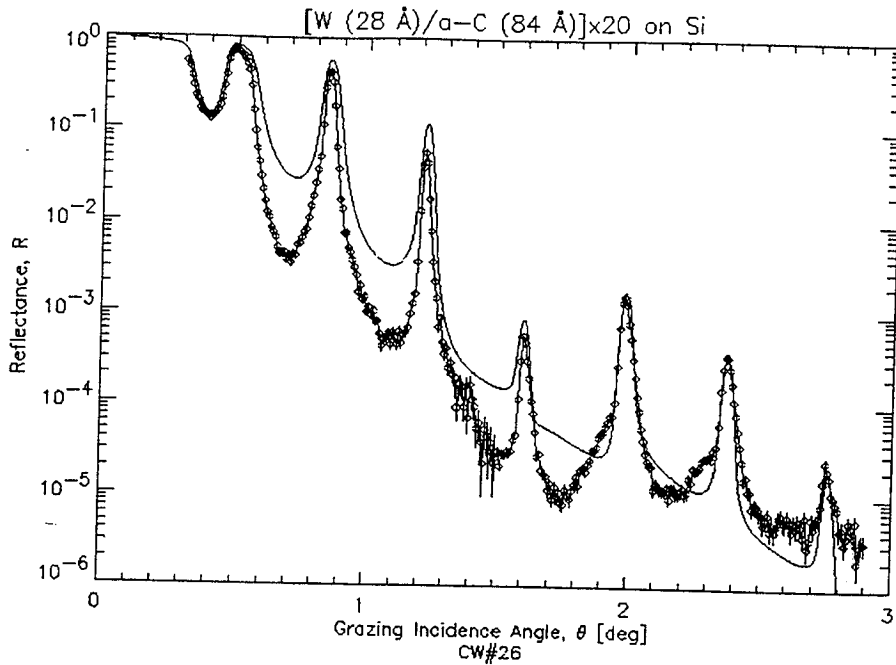


Figure 1: Measured and fitted reflectance scans for sample CW#26 ($N=20$ bilayers, $d(\text{fit})=113 \text{ \AA}$, $\gamma(\text{fit})=0.254$). A collimated beam of 8.048 keV ($\text{Cu K}\alpha$ radiation) incident at grazing angle θ on the sample was detected by a collimated $\text{NaI}(\text{Tl})$ detector positioned at 2θ relative to the beam direction.

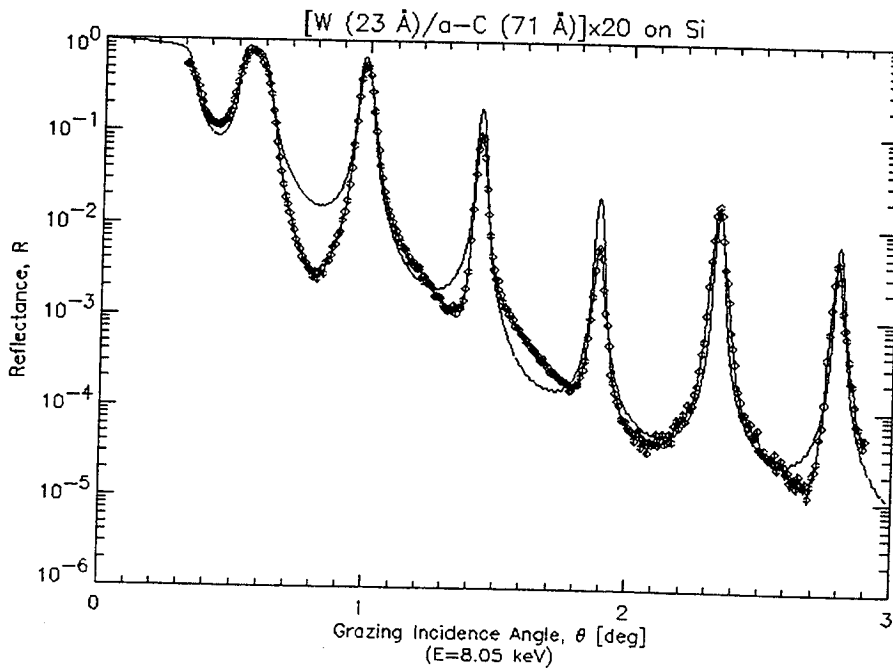


Figure 2: Measured and fitted reflectance scans for sample CW#27 ($N=20$ bilayers, $d(\text{fit})=95 \text{ \AA}$, $\gamma(\text{fit})=0.250$).

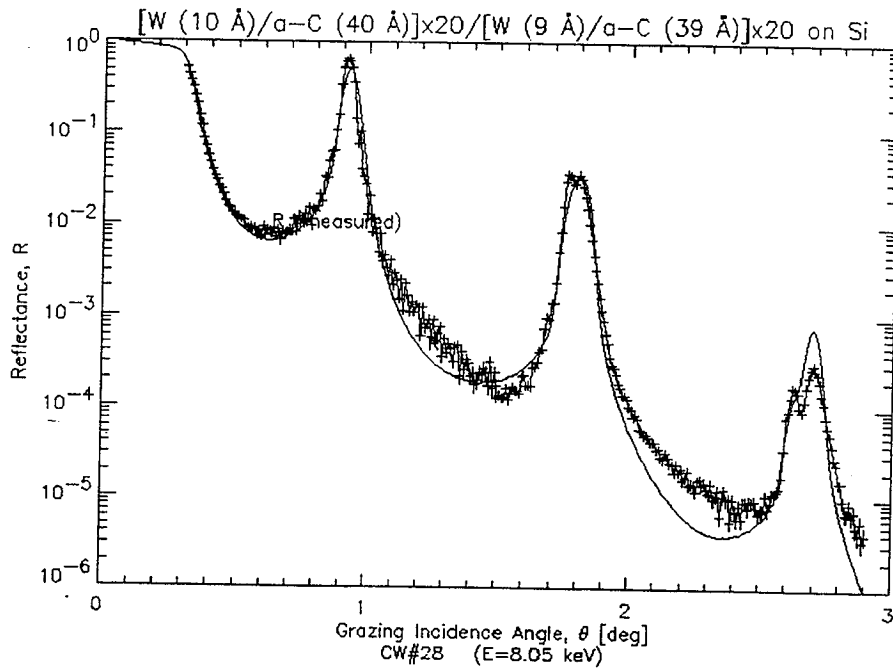


Figure 3: Measured and fitted reflectance scans for sample CW#28 (N=40 bilayers, $d(\text{fit})=51 \text{ \AA}$, $\gamma(\text{fit})=0.203$)

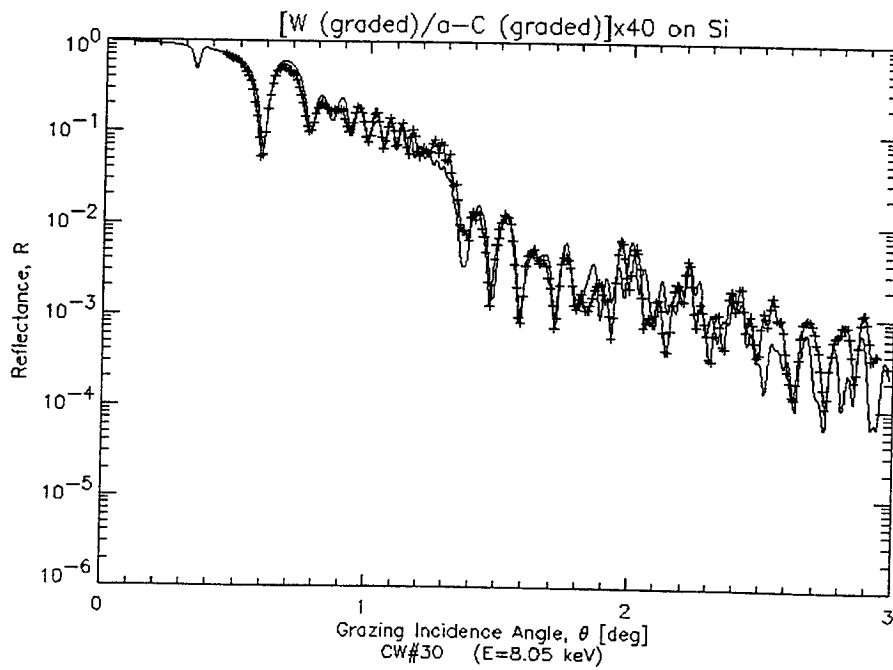


Figure 4: Measured and fitted reflectance scans for sample CW#30 (N=40 bilayers, graded $d(\text{fit})=160 \text{ \AA}$ to 36 \AA , $\gamma(\text{fit})=0.368$)

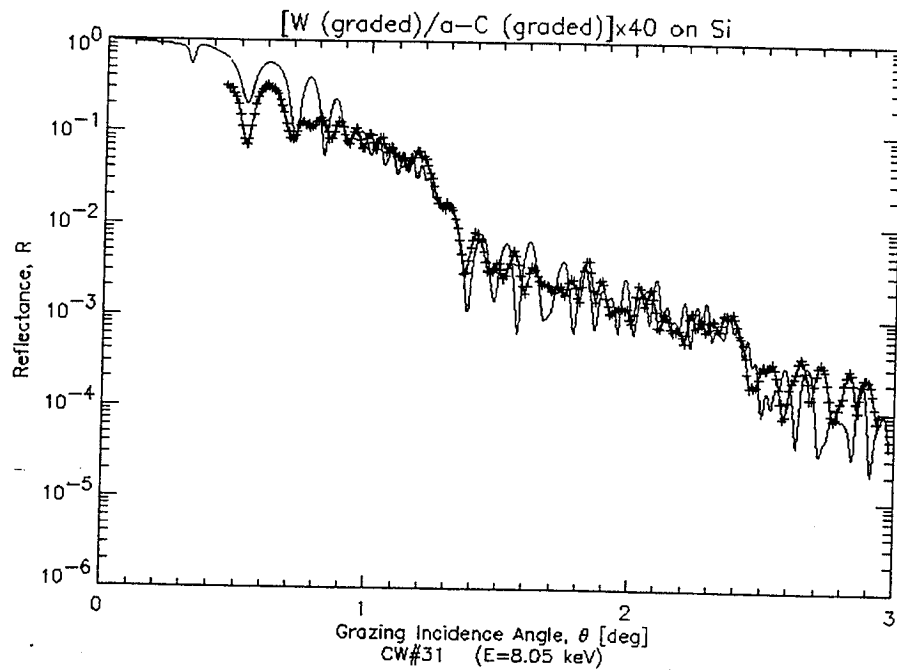


Figure 5: Measured and fitted reflectance scans for sample CW#31 (N=40 bilayers, graded $d(\text{fit})=180 \text{ \AA}$ to 36 \AA , $\gamma(\text{fit})=0.366$)

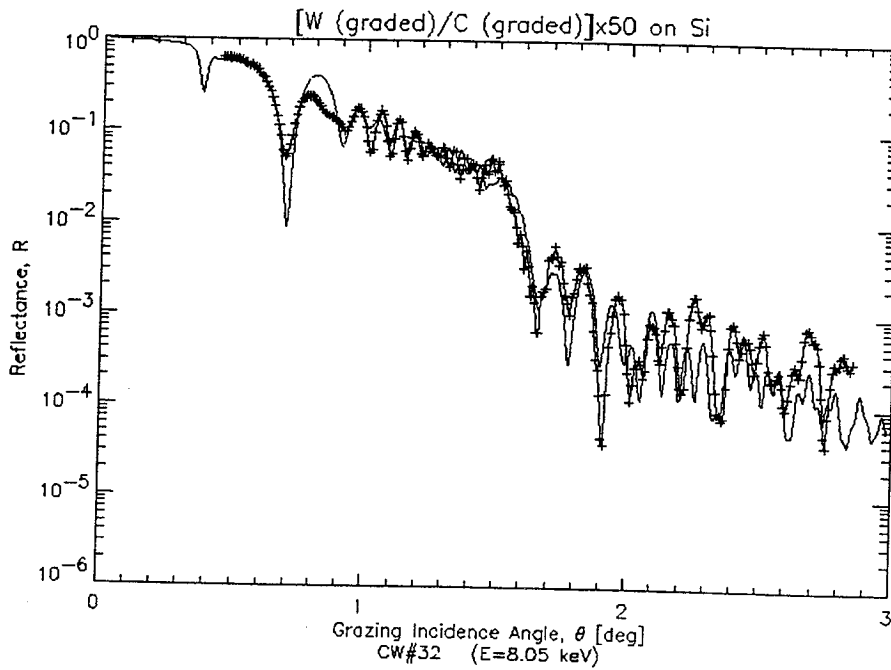


Figure 6: Measured and fitted reflectance scans for sample CW#32 (N=50 bilayers, graded $d(\text{fit})=126 \text{ \AA}$ to 28 \AA , graded $\gamma(\text{fit})=0.340$ to 0.439)

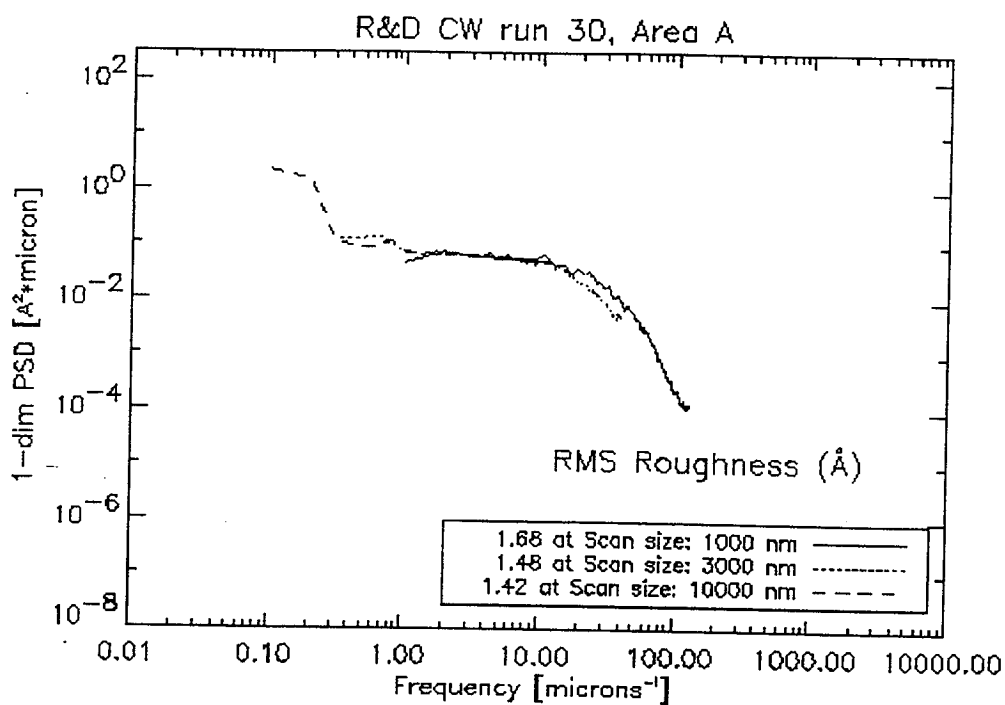


Figure 7: Power spectral density plots of the AFM scans of sample CW#30. Three different scan sizes were used ($1\ \mu\text{m}$, $3\ \mu\text{m}$, and $10\ \mu\text{m}$) to probe different frequency ranges. The rms microroughness is $\approx 1.5\ \text{\AA}$.

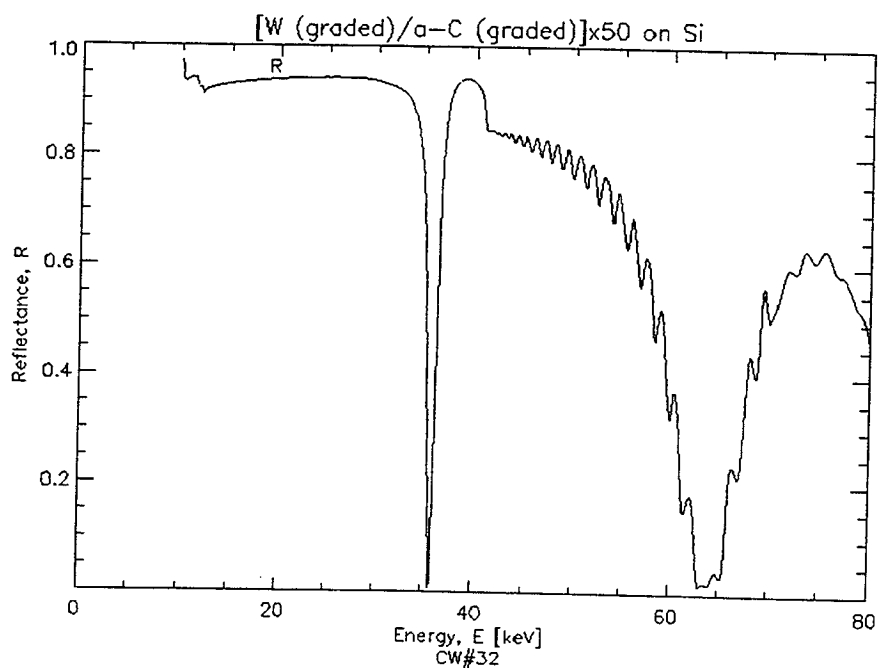


Figure 8: Calculated reflectance vs. energy for CW32 at fixed grazing incidence angle $\theta=5\ \text{arcmin}$.